Journal of Computer Science and Cybernetics, V.40, N.1 (2024), 1–22
DOI no. 10.15625/1813-9663/19218

REVIEW

50 YEARS FIELD ORIENTED CONTROL OF THREE-PHASE AC DRIVES IN THE PRACTICE - THE STATE-OF-THE-ART

NGUYEN PHUNG QUANG

Institute for Control Engineering and Automation, Hanoi University of Science and Technology, 01 Dai Co Viet Street, Hai Ba Trung District, Ha Noi, Viet Nam

Abstract. From DC motors (DCM) we know, it is possible to independently control the two currents of the flux and torque generating. Because the two DCM circuits are completely isolated, we obtain simple adjustment algorithms that require little computing time on the microprocessor. For this reason, DCM has been at the forefront of the application of digital controls in drive control systems in the early years, especially in high-performance systems. On the contrary, the three-phase AC motor (ACM) has a complex structure due to the winding system and three-phase power supply, and has caused significant difficulties in the mathematical description of the above decoupling characteristics. The purpose of the field-oriented control (FOC) is therefore to create a tool that allows the decoupling control of the flux and torque-producing current components from the three-phase AC currents flowing in the coil. The FOC drive system is a system based on the principle of decoupling the above power components thanks to the stator current feedback control (the innermost circuit of the drive system). The FOC-type control method belongs to the class of vector control methods for electrical machines.

On the occasion of the 50th anniversary of FOC, this paper aims to provide an overview of the development status of FOC in industrial practice. The content presented deals mainly with 3-phase induction motors.

Keywords. Three-phase AC motor, IM, FOC, field oriented control, direct FOC, indirect FOC, linear control, nonlinear control, exact linearization, flatness-based control.

Abbreviations

ACM	AC Motor
DCM	DC Motor
FOC	Field oriented control
IM	Induction motor
IGBT	Insutaled-Gate Bipolar Transistor
MOSFET	Metal-Oxide-Semiconductor Field-Effect Transistor
RFOC	Rotor Flux Oriented Control

Corresponding author.
E-mail addresses: quang.nguyenphung@hust.edu.vn

1. INTRODUCTION

"*Electric drives*" is not just a scientific and technological field with a long history. Since its invention 200 years ago, the electric motor has always played an important role in promoting the development of human society through "*electrification*" and "*automation*". Today, 200 years later, in the era of "*digitalization*" of all social activities, in the era of the 4th industrial revolution, the role of "*electric drives*" has not diminished, but is even more important: they have become "*intelligent actuators*" of production lines, of robot chains, of autonomous vehicles, etc., which can be accessed and controlled from anywhere on earth.

Throughout the development of three-phase AC drives, the term FOC, representative of the modeling and control method, cannot be separated. The idea called FOC first appeared in [1]. It was not until [2] that the FOC concept was confirmed as an official method, which has just turned 50 years old. Although FOC was "honoured and confirmed" by its master, professor Leonhard [3], this paper boldly sets out to "illuminate" the 50 years that FOC has been around.

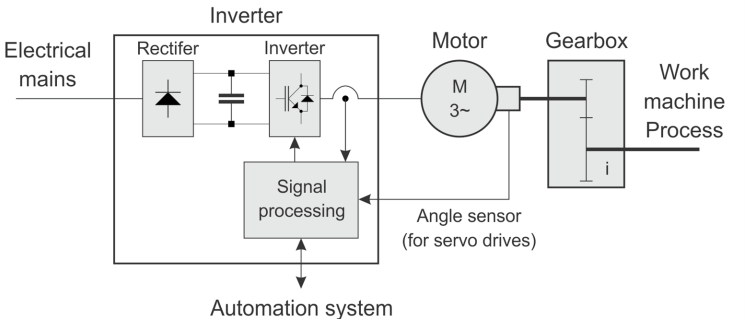

Figure 1: Structure of a drive system in the practice [4]

Controlled three-phase drive systems (Figure 1), consisting of frequency converters or servo drives and three-phase motors, are currently the most economical choice for drive systems with power ratings above 100 W that can be used in automatic production [4]. The advantage of these systems is the possibility of direct power supply via the mains without the need for a transformer. The basis of this technology is the introduction of powerful, switchable semiconductor valves (IGBT, MOSFET) and microcontrollers with high computing power.

Low-voltage drives (small permanently excited DC motors, stepper motors) have a predominant share of low power. DC motors with thyristor power supply have been replaced by regulated three-phase drives, as three-phase drives require less maintenance and are cheaper.

1.1. Three-phase quantities as vector and choice of the coordinate system

After the introductory words, the question to be clarified includes two topic groups "FOC and FOC structure (Figure 1)" for controlling a 3-phase AC motor. To understand FOC, we actually just need to understand and remember the knowledge in the following 4 steps.

1.1.1. Step 1: Three-phase quantities as complex vectors

All 3-phase AC quantities of the motor are converted into a complex vector representation. The 3-phase stator current is now considered in more detail as an example. The three sinusoidal phase

currents i_{su}, i_{sv}, and i_{sw} of a star-point insulated three-phase machine fulfill the following relationship

$$i_{su}(t) + i_{sv}(t) + i_{sw}(t) = 0. \tag{1}$$

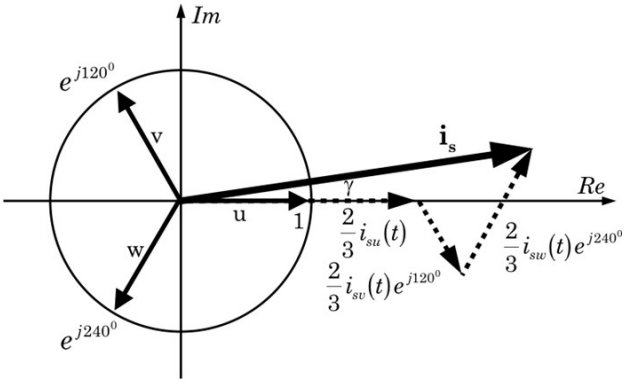

Figure 2: Transformation of the phase currents into the current vector

The complex vector results from formula (2). The transformation of other quantities such as the voltages $\mathbf{u_s}$, $\mathbf{u_r}$, and flux Ψ_s, Ψ_r is carried out similarly.

$$\mathbf{i_s} = \frac{2}{3}\left[i_{su}(t) + i_{sv}(t)e^{j\gamma} + i_{sw}(t)e^{j2\gamma}\right] \text{ with } \gamma = 2\pi/3. \tag{2}$$

Complex vectors like formula (2) can be represented in different Cartesian coordinate systems. However, only those systems that can demonstrate advantages in terms of modeling and controller design should be considered.

1.1.2. Step 2: Choice of rotor flux oriented dq-coordinate system

However, only those systems that can demonstrate advantages in terms of modeling and controller design should be considered. The choice of the coordinate system means defining the real axis to a concrete vector. In this case, it is the rotor flux vector (Figure 3). The term FOC now becomes RFOC.

Figure 3 indicates that successful rotor flux orientation requires precise knowledge of the rotor flux Ψ_r and flux orientation angle θ_s (Figure 4). If the rotor flux linkage is to be kept constant using control, an actual value recording is necessary in any case.

- Since a *direct measurement* (the so-called *direct FOC*) of the rotor flux linkage requires the installation of measuring sensors in the motor and, in addition, no useful measured values are available at very low speeds.
- An *indirect actual value recording* (the so-called *indirect FOC*) of the rotor flux linkage with the aid of a flux model (FM) is usually provided in connection with digital controls. This approach is predominantly used in practice. Instead of a flux model, a Luenberger observer or a Kalman filter can also be used advantageously.

The stator current $\mathbf{i_s}$ in the stator coordinate system and the mechanical angular velocity ω of the motor are measured.

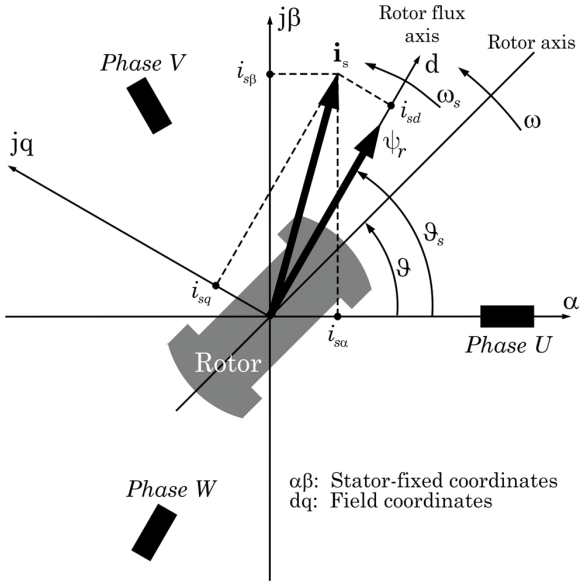

Figure 3: Stator current vector of IM in stator-fixed and field coordinates

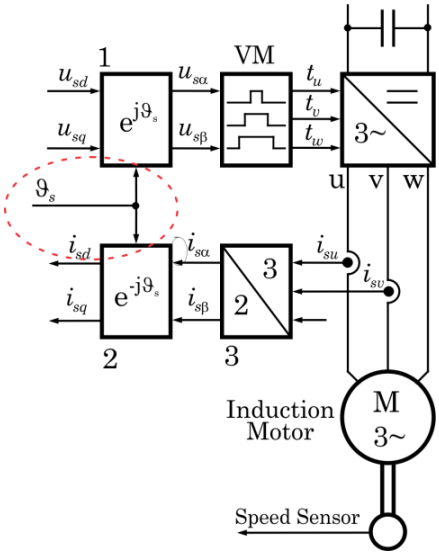

Figure 4: Interface between control, inverter, and motor (1, 2: Park transformation; 3: Clarke transformation)

1.1.3. Step 3: Advantages of chosen RFOC dq-coordinate system

If the real axis d of the coordinate system (Figure 3) corresponds to the direction of the rotor flux Ψ_r, a physically easily understandable representation of the relationships between torque, flux, and current components is obtained. These relationships look like the formula (3)

$$y_{rd}(s) = \frac{L_m}{1+sT_r} i_{sd}, \; m_M = \frac{3}{2}\frac{L_m}{L_r} z_p \psi_{rd} i_{sq}. \tag{3}$$

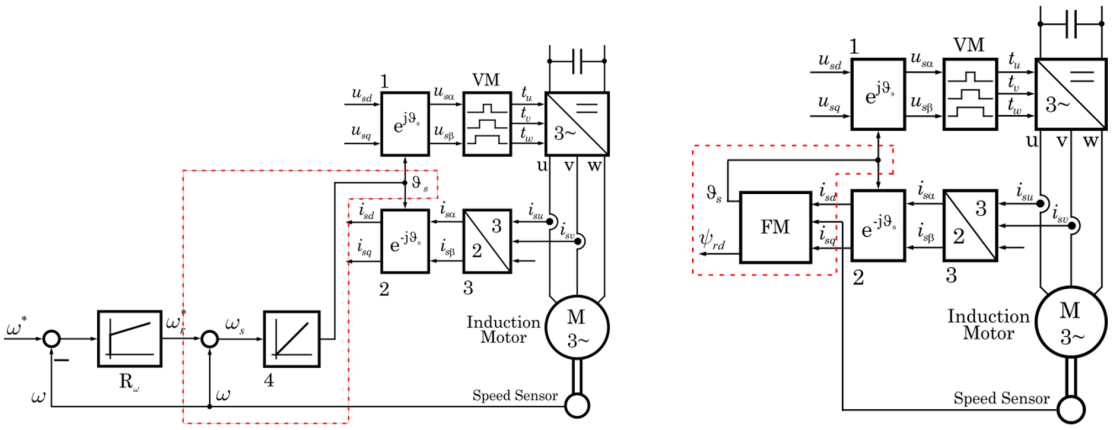

Figure 5: The concept of direct FOC (left) and indirect FOC (rights) to obtain the flux angle θ_s

Formula (3) shows the flux-forming effect of i_{sd} and the moment-forming effect of i_{sq}. These decoupled effects between isd and isq lead to the following important conclusion in step 4. After 50 years of "research - development - production", you can now clearly see the trend that indirect FOC dominates (Figure 6) in industrial practical implementations.

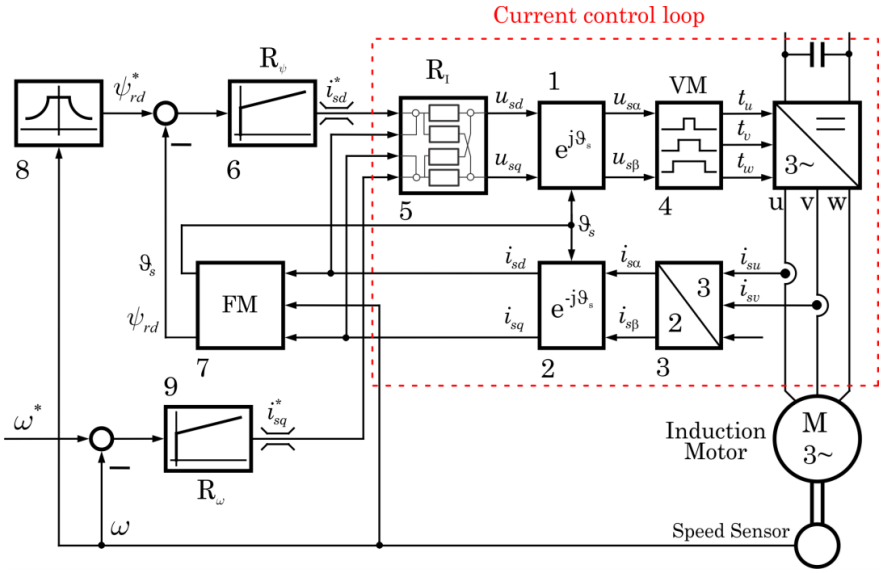

Figure 6: The concept of indirect FOC dominates in practice

1.1.4. Step 4: Conclusion

If the innermost control loop (current vector control) guarantees the control performance "quickly - exactly - decoupled", then it is possible to design the outer control loops (flux, speed) as in the drive system with externally excited DC motors.

We can assume that the 3-phase AC motor is powered by a current source inverter (CSI) that ensures the supply of two current components i_{sd} and i_{sq} according to the system requirements.

1.2. Introduction outlook

In reality, the induction motor is an object with a complex mathematical model. There are dynamic interactions between the dq-axis components of the stator current. Canonically, we must consider the motor as a two-dimensional control object. Therefore, this object can be well controlled only with a two-dimensional control matrix. In the structure of this control matrix (Figure 6: block $\mathbf{R_I}$), besides the components lying on the diagonal (main branch), there are also components lying off the diagonal (branch with decoupling effect), which ensure the elimination of interaction effects.

At this point, we can say that although today, after 50 years, we have many methods at our disposal to design $\mathbf{R_I}$ controllers, we still have to adhere to the requirements of "quickly - exactly - decoupled" (see [3, 5–7]).

2. MACHINE MODELS

According to [8], the IM is described by the following system

$$\begin{cases} \mathbf{u}_s^f = R_s \mathbf{i}_s^f + \dfrac{d\psi_s^f}{dt} + j\omega_s\, \psi_s^f \\ \mathbf{0} = R_r\, \mathbf{i}_r^f + \dfrac{d\psi_r^f}{dt} + j\omega_r\, \psi_r^f \\ \psi_s^f = L_s\, \mathbf{i}_s^f + L_m\, \mathbf{i}_r^f \\ \psi_r^f = L_m\, \mathbf{i}_s^f + L_r\, \mathbf{i}_r^f. \end{cases} \tag{4}$$

The system (4) can also be written in component notation as follows

$$\begin{cases} \dfrac{di_{sd}}{dt} = -\left(\dfrac{1}{\sigma\, T_s} + \dfrac{1-\sigma}{\sigma\, T_r}\right) i_{sd} + \omega_s\, i_{sq} + \dfrac{1-\sigma}{\sigma\, T_r}\psi'_{rd} + \dfrac{1-\sigma}{\sigma}\omega\psi'_{rq} + \dfrac{1}{\sigma\, L_s}u_{sd} \\ \dfrac{di_{sq}}{dt} = -\omega_s\, i_{sd} - \left(\dfrac{1}{\sigma\, T_s} + \dfrac{1-\sigma}{\sigma\, T_r}\right) i_{sq} - \dfrac{1-\sigma}{\sigma}\omega\psi'_{rd} + \dfrac{1-\sigma}{\sigma\, T_r}\psi'_{rq} + \dfrac{1}{\sigma\, L_s}u_{sq} \\ \dfrac{d\psi'_{rd}}{dt} = \dfrac{1}{T_r} i_{sd} - \dfrac{1}{T_r}\psi'_{rd} + (\omega_s - \omega)\ \psi'_{rq} \\ \dfrac{d\psi'_{rq}}{dt} = \dfrac{1}{T_r} i_{sq} - (\omega_s - \omega)\ \psi'_{rd} - \dfrac{1}{T_r}\psi'_{rq}. \end{cases} \tag{5}$$

Figure 7 shows an easy-to-understand IM model in the dq coordinate system.

2.1. State-space models of IM ([8])

For better access to control concepts, the state model of the control objects is used. The system (5) is rewritten for this purpose.

2.1.1. Continuous state space models

$$\begin{aligned} &\frac{d\mathbf{x}^f}{dt} = \mathbf{A}^f\, \mathbf{x}^f + \mathbf{B}^f\, \mathbf{u}_s^f + \mathbf{N}\, \mathbf{x}^f\, \omega_s, \\ &\mathbf{x}^{f\,T} = \left[i_{sd},\, i_{sq},\, \psi'_{rd},\, \psi'_{rq}\right],\ \mathbf{u}_s^{f\,T} = \left[u_{sd},\, u_{sq}\right], \end{aligned} \tag{6}$$

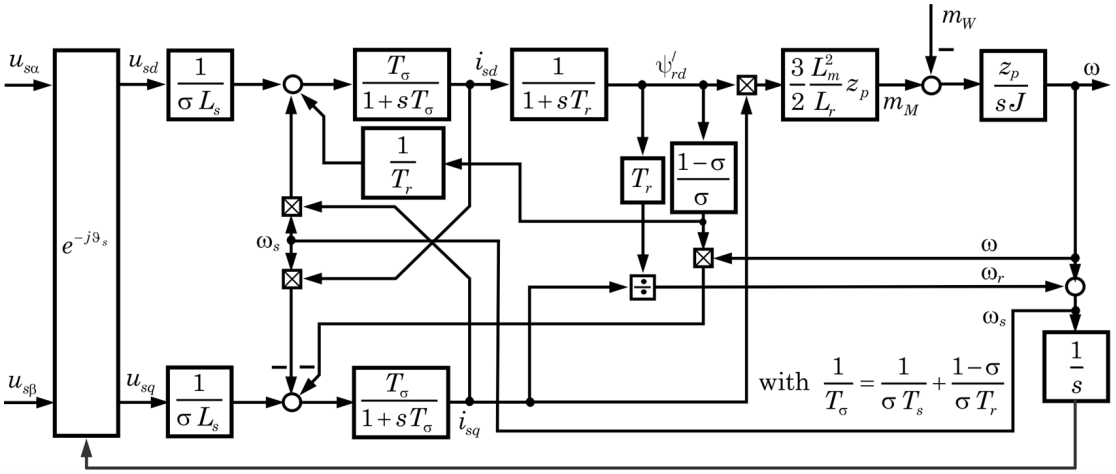

Figure 7: Model of the IM in field synchronous dq coordinate system

with the state vector $\mathbf{x}^f$, the input vector $\mathbf{u}_s^f$

$$\mathbf{A}^f = \left[\begin{array}{cc|cc} -\left(\frac{1}{\sigma T_s}+\frac{1-\sigma}{\sigma T_r}\right) & 0 & \frac{1-\sigma}{\sigma T_r} & \frac{1-\sigma}{\sigma}\omega \\ 0 & -\left(\frac{1}{\sigma T_s}+\frac{1-\sigma}{\sigma T_r}\right) & -\frac{1-\sigma}{\sigma}\omega & \frac{1-\sigma}{\sigma T_r} \\ \hline \frac{1}{T_r} & 0 & -\frac{1}{T_r} & -\omega \\ 0 & \frac{1}{T_r} & \omega & -\frac{1}{T_r} \end{array}\right], \tag{7}$$

$$\mathbf{B}^f = \left[\begin{array}{cc} \frac{1}{\sigma L_s} & 0 \\ 0 & \frac{1}{\sigma L_s} \\ \hline 0 & 0 \\ 0 & 0 \end{array}\right], \quad \mathbf{N} = \left[\begin{array}{cc|cc} 0 & 1 & 0 & 0 \\ -1 & 0 & 0 & 0 \\ \hline 0 & 0 & 0 & 1 \\ 0 & 0 & -1 & 0 \end{array}\right].$$

The system (6) is *bilinear*. Here, the components u_{sd}, and u_{sq} of the stator voltage and the angular velocity ω_s of the stator circuit are input quantities. Figure 8 illustrates the derived state model with their bilinearity.

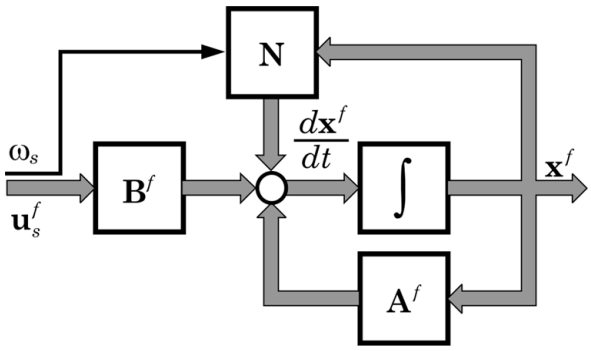

Figure 8: State space model of the IM in dq coordinates

2.1.2. Discrete state space models

From the early days of the FOC idea, we knew that the future of FOC would definitely involve microcontrollers. Thirty years ago (see [3, 6, 7]) we saw the evidence and now it is confirmed. For this, we need appropriate starting points. These are the discrete state models.

According to [8], the model has the following form

$$\mathbf{x}^f(k+1) = \Phi^f \mathbf{x}^f(k) + \mathbf{H}^f \mathbf{u}_s^f(k). \tag{8}$$

Equation (8) can be rewritten into (9) using submatrices to clearly show the role of each submodel. From (8) we obtain the following two submodels like (9), illustrated in Figure 9a.

$$\begin{cases} \mathbf{i}_s^f(k+1) = \Phi_{11}^f \mathbf{i}_s^f(k) + \Phi_{12}^f \psi_r^{f/}(k) + \mathbf{H}_1^f \mathbf{u}_s^f(k) \\ \psi_r^{f/}(k+1) = \Phi_{21}^f \mathbf{i}_s^f(k) + \Phi_{22}^f \psi_r^{f/}(k). \end{cases} \tag{9}$$

The technical, physical characteristics of the motor, shown in Figure 9a, state:

- The motor model includes two submodels as in formula (9) and Figure 9a.
- The upper submodel, the first equation in formula (9) or Figure 9b, represents the stator current model $\mathbf{i_s}$ required for the controller design.
- The lower submodel, the second equation in formula (9) or Figure 9c, represents the rotor flux model ψ_r required for the design of flux calculation (for example, Luenberger observer or Kalman filter).

2.2. Nonlinear properties of the IM models ([8])

Due to their complex mechanical structure with a magnetic circuit containing many winding slots and air gaps, 3-phase AC machines exhibit many different non-linear characteristics. However, there are only two nonlinear properties that play an important role in control system design:

- *The nonlinear structure of the process models:* This nonlinearity is caused by products between state variables like current components i_{sd}, i_{sq}, and input variable ω_s.
- *The nonlinear parameters:* Some parameters like the mutual inductance L_m depend on the rotor flux which is a state variable.

This article only introduces two possible methods in practice: Control using exact linearization and control based on flat characteristics of the object. These are two methods that help overcome nonlinear structural characteristics, allowing the design of nonlinear controllers to improve control quality in complex operating modes.

2.2.1. Idea of the exact linearization using state coordinate transformation

The basic idea of the *exact linearization* ([9, 10]) can be shortly summarized as follows: If the nonlinear MIMO system in the form (10)

$$\begin{cases} \dfrac{d\mathbf{x}}{dt} = \mathbf{f}(\mathbf{x}) + \mathbf{H}(\mathbf{x})\,\mathbf{u} \\ \mathbf{y} = \mathbf{g}(\mathbf{x}), \end{cases} \tag{10}$$

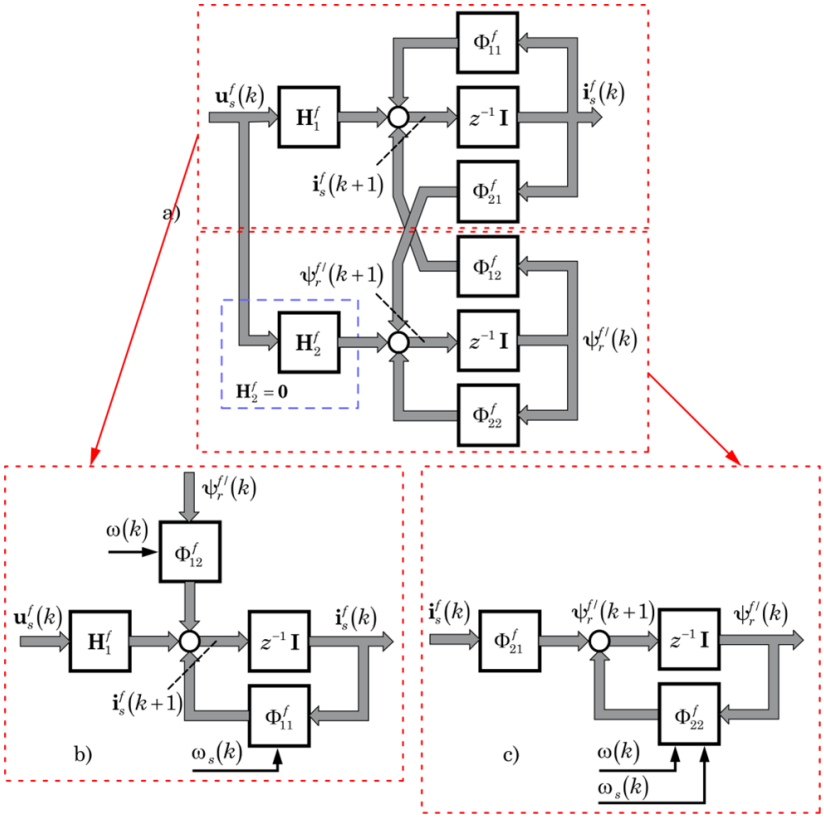

Figure 9: Discrete state space model of the IM in *dq* coordinates

belongs to the class of processes with a vector of *relative difference orders*, the condition for exact linearization ([8]), then the system (10) can be transformed using the coordinate transformation (11)

$$\mathbf{z} = \begin{pmatrix} z_1 \\ \vdots \\ z_n \end{pmatrix} = \mathbf{m}(\mathbf{x}) = \begin{pmatrix} m_1^1(\mathbf{x}) \\ \vdots \\ m_{r_1}^1(\mathbf{x}) \\ \vdots \\ m_1^m(\mathbf{x}) \\ \vdots \\ m_{r_m}^m(\mathbf{x}) \end{pmatrix} = \begin{pmatrix} g_1(\mathbf{x}) \\ \vdots \\ L_f^{r_1-1} g_1(\mathbf{x}) \\ \vdots \\ g_m(\mathbf{x}) \\ \vdots \\ L_f^{r_m-1} g_m(\mathbf{x}) \end{pmatrix} \tag{11}$$

into the following linear MIMO system

$$\begin{cases} \dfrac{d\mathbf{z}}{dt} = \mathbf{A}\mathbf{z} + \mathbf{B}\mathbf{w} \\ \mathbf{y} = \mathbf{C}\mathbf{z}. \end{cases} \tag{12}$$

The original input $\mathbf{u}$ is then controlled by the coordinate transformation law

$$\mathbf{u} = \mathbf{a}(\mathbf{x}) + \mathbf{L}^{-1}(\mathbf{x})\,\mathbf{w}. \tag{13}$$

The vector $\mathbf{a}(\mathbf{x})$ and the matrix $\mathbf{L^{-1}}(\mathbf{x})$ in (13) look as follows

$$\mathbf{L}\left(\mathbf{x}\right)=\begin{pmatrix} L_{h_1}L_f^{r_1-1}g_1\left(\mathbf{x}\right) & \cdots & L_{h_m}L_f^{r_1-1}g_1\left(\mathbf{x}\right) \\ \vdots & \ddots & \vdots \\ L_{h_1}L_f^{r_m-1}g_m\left(\mathbf{x}\right) & \cdots & L_{h_m}L_f^{r_m-1}g_m\left(\mathbf{x}\right) \end{pmatrix},\ \mathbf{a}\left(\mathbf{x}\right)=-\mathbf{L}^{-1}\left(\mathbf{x}\right)\begin{pmatrix} L_f^{r_1}g_1\left(\mathbf{x}\right) \\ \vdots \\ L_f^{r_m}g_m\left(\mathbf{x}\right) \end{pmatrix}. \tag{14}$$

Formula (14) also requires the ability, concerning the coordinate transformation or the exact linearization, to invert the matrix $\mathbf{L}(\mathbf{x})$. In equations (11) and (14), the term

$$L_f g\left(\mathbf{x}\right)=\frac{\partial g\left(\mathbf{x}\right)}{\partial \mathbf{x}}\mathbf{f}\left(\mathbf{x}\right), \tag{15}$$

notifies the Lie derivation of the function $g(\mathbf{x})$ along the trajectory $\mathbf{f}(\mathbf{x})$. Following equation (12) the process is now linear in the new state space $\mathbf{z}$ so that only a linear controller must be designed (Figure 10). Besides the exact linearization, the *input-output decoupling* (decoupling between both axes *dq*) *relations are totally guaranteed.* The so-called concept of *direct decoupling* is dynamically effective for the complete state space.

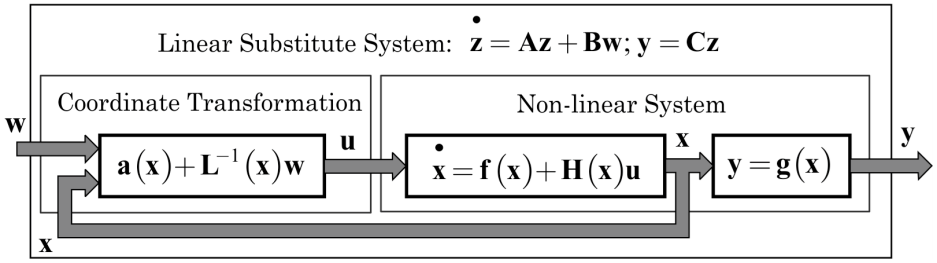

Figure 10: Concept of exact linearized process model ([8])

2.2.2. Flatness and the idea of the flatness-based control design

The concept of flat systems was introduced in [9,10]. Specific application instructions for IM drive systems can be found in [8]. The application of the idea of flat systems can be re-iterated shortly as follows.

Given is the following nonlinear system

$$\frac{d\mathbf{x}}{dt}=f\left(\mathbf{x},\mathbf{u}\right), \tag{16}$$

with $\dim\mathbf{x}=n,\ \dim\mathbf{u}=m<n$ and $\operatorname{rank}\left(\partial f/\partial\mathbf{u}\right)=m$. The system (16) is differentially flat, or shortly flat, if the two following conditions are fulfilled:

- Condition 1: There exists an output vector $\mathbf{y}$ and finite integers l and r such that

$$\mathbf{y}=\begin{bmatrix} y_1 \\ \vdots \\ y_m \end{bmatrix}=F\left(\mathbf{x},\mathbf{u},\frac{d\mathbf{u}}{dt},...,\frac{d^l\mathbf{u}}{dt^l}\right). \tag{17}$$

- Condition 2: Both input vector $\mathbf{u}$ and state vector $\mathbf{x}$ can be expressed in function of $\mathbf{y}$ and its successive derivatives in finite number

$$\mathbf{x} = P\left(\mathbf{y}, \frac{d\mathbf{y}}{dt}, ..., \frac{d^r\mathbf{y}}{dt^r}\right), \ \mathbf{u} = Q\left(\mathbf{y}, \frac{d\mathbf{y}}{dt}, ..., \frac{d^{(r+1)}\mathbf{y}}{dt^{(r+1)}}\right), \tag{18}$$

with $dP/dt = f(P, Q)$. The output vector $\mathbf{y}$ is called a flat output. The 2nd equation in (18) is also called the "inverse" process model of the system (16) with the output (17). According to (17) and (18) it can be concluded that to every output trajectory $t \mapsto \mathbf{y}(t)$ being enough differentiable, there corresponds a state and input trajectory

$$t \mapsto (\mathbf{x}(t), \mathbf{u}(t)) = \left(P\left(\mathbf{y}, \frac{d\mathbf{y}}{dt}, ..., \frac{d^r\mathbf{y}}{dt^r}\right), Q\left(\mathbf{y}, \frac{d\mathbf{y}}{dt}, ..., \frac{d^{(r+1)}\mathbf{y}}{dt^{(r+1)}}\right)\right), \tag{19}$$

that identically satisfies the system equations. Conversely, to every state and input trajectory $t \mapsto (\mathbf{x}(t), \mathbf{u}(t))$ being enough differentiable and satisfying the system equations, a trajectory

$$t \mapsto \mathbf{y}(t) = F\left(\mathbf{x}, \mathbf{u}, \frac{d\mathbf{u}}{dt}, ..., \frac{d^l\mathbf{u}}{dt^l}\right), \tag{20}$$

should correspond. In the case that both conditions (17), (18) are fulfilled, and the system (16) and its output vector (17) are flat, we can figure out a general control structure as in Figure 11 which is engineer-friendly and easier to understand as the original nonlinear system.

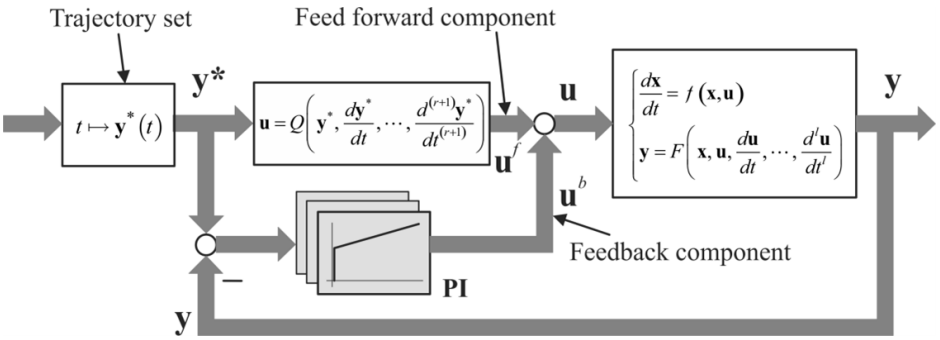

Figure 11: The general flatness-based control structure ([8])

The operation of the concept in Figure 11 can be summarized as follows:

- If the process satisfies the conditions of flatness, the inverse model of the process may be used as a feed-forward component $\mathbf{u}^f$ of a tracking control concept.
- The forward component $\mathbf{u}^f$ is effective only when the input signal $\mathbf{y}^*$ is so often differentiable like the output signal $\mathbf{y}$ of the process. Therefore, the use of a trajectory set for $\mathbf{y}^*$ is absolutely necessary.
- Thus, the output signal $\mathbf{y}$ in the case of the perturbed system to the input signal $\mathbf{y}^*$ along the trajectory exactly follows and the steady-state error is eliminated in the new position of rest, a third component $\mathbf{u}^b$ is still needed as feedback. In the case of electrical machines, PI controllers will be sufficient.

3. FAST TORQUE IMPRESSION USING DYNAMIC CURRENT FEEDBACK CONTROL

Equation (3) and Figure 6 clearly state that an indirect FOC-based current control loop with the performance "fast - exact - decoupled" is absolutely necessary to turn the "inverter - motor" combination into an actuator. The linear controllers are varied and have been presented several times (see [6, 7, 9, 11–13]).

3.1. Linear controller design

Figure 12 shows the process model with the compensation of the disturbance variable ψ_r and the dead time effect of the inverter.

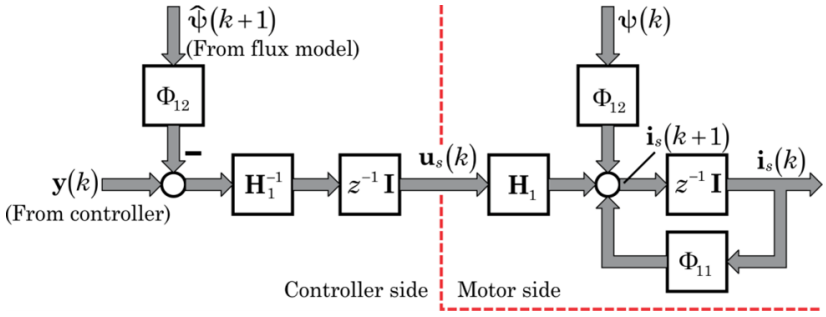

Figure 12: The general compensated process model $\mathbf{i}_s$ ([8])

Despite the variety of variants, the controller design basically uses the block structure presented in Figure 13. The design in the state space is presented in Figure 14.

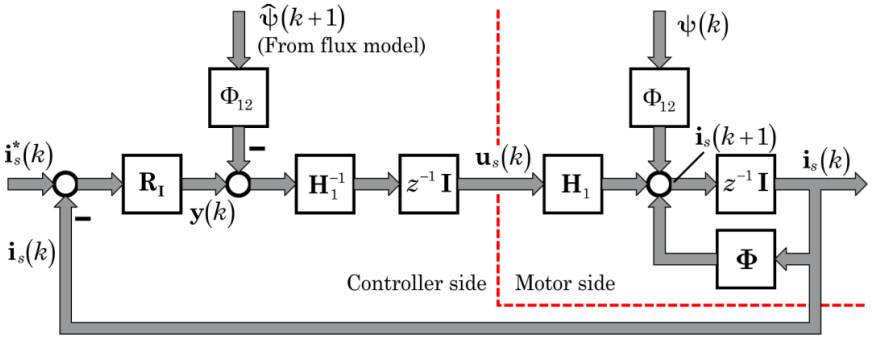

Figure 13: Block structure of the current vector controller for IM ([8])

The latest and probably best variant $\mathbf{R}_I$ in terms of starting behavior and accuracy was presented in [13]. The design uses the following process model (21)) in Figure 9b (the 1st equation of (9))

$$\mathbf{i}_s\,(k+1) = \Phi_{11}\,\mathbf{i}_s\,(k) + \Phi_{12}\,\psi_r'\,(k) + \mathbf{H}_1\,\mathbf{u}_s\,(k)\,. \tag{21}$$

The result is the following equation

$$\mathbf{R}_I(z) = \mathbf{A}(z)\,\mathbf{L}\left(z^{-1}\right)\left[\mathbf{I} - z^{-1}\mathbf{L}\left(z^{-1}\right)\right]^{-1} = \begin{bmatrix} \dfrac{(z-\Phi_{11})\,L_1\left(z^{-1}\right)}{1-z^{-1}L_1\left(z^{-1}\right)} & \dfrac{-\Phi_{12}L_2\left(z^{-1}\right)}{1-z^{-1}L_2\left(z^{-1}\right)} \\ \dfrac{\Phi_{12}L_1\left(z^{-1}\right)}{1-z^{-1}L_1\left(z^{-1}\right)} & \dfrac{(z-\Phi_{11})\,L_2\left(z^{-1}\right)}{1-z^{-1}L_2\left(z^{-1}\right)} \end{bmatrix}. \tag{22}$$

In equation (22), the matrix $\mathbf{A}$ plays the role of a system matrix

$$\mathbf{A}(z) = z\mathbf{I} - \mathbf{\Phi} \text{ with } \det\mathbf{A} = \left(z - 1 + \frac{T}{\sigma}\left(\frac{1}{T_s} + \frac{1-\sigma}{T_r}\right)\right)^2 + (\omega_s T)^2 > 0. \tag{23}$$

Only the matrix of polynomials $\mathbf{L}$ must be found

$$\mathbf{L}\left(z^{-1}\right) = \begin{bmatrix} L_1\left(z^{-1}\right) & 0 \\ 0 & L_2\left(z^{-1}\right) \end{bmatrix}. \tag{24}$$

The terms $L_1(z^{-1})$ and $L_2(z^{-1})$ are polynomials of n_1-th and n_2-th degrees, then the current components i_{sd} and i_{sq} will follow their set points after exactly n_1+1 and n_2+1 sampling periods.

A very interesting variant is the current control in the state space in Figure 14. More details about the design can be found in [8]. The specific design steps for both structures can be found in [9].

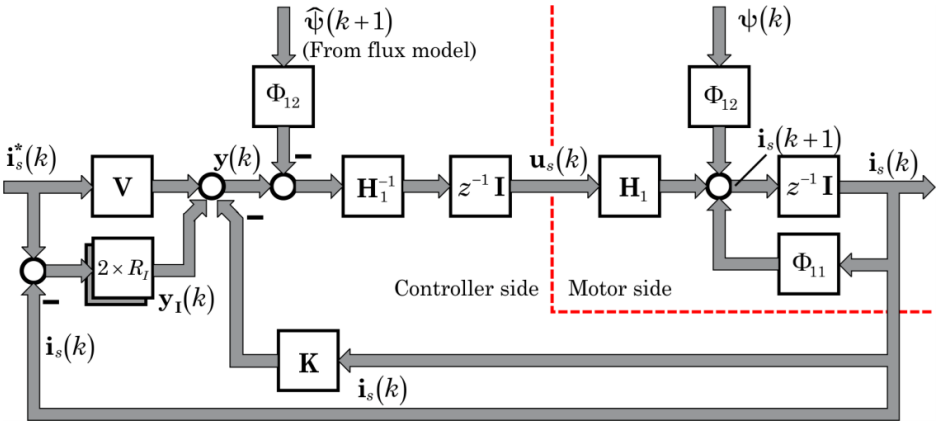

Figure 14: Block structure of the current vector controller in state space ([8])

However, some specific features should be mentioned here.

- The structure in Figure 13 is characterized by its robustness. This is a big advantage for systems during automatic self-identification and self-commissioning.
- On the contrary, the structure in Figure 14 requires more precise data, but is characterized by high accuracy. The torque ripple is very small. For high-quality drives, the additional effort compensates for the additional costs of data procurement.

3.2. Nonlinear controller design

3.2.1. Control using exact linearization

Now it seems possible to replace the two-dimensional current controller (Figure 6) with a coordinate transformation and two separate current controllers for both axes dq (Figure 15).

The direct decoupling concept in Figure 15 is dynamically effective for the entire state space. The two current controllers R_{Isd} and R_{Isq} do not need to have PI characteristics and can be designed with modern algorithms such as dead-beat control. A dynamic and almost delay-free imprinting of the motor torque can be ensured without interrupting a linearization condition.

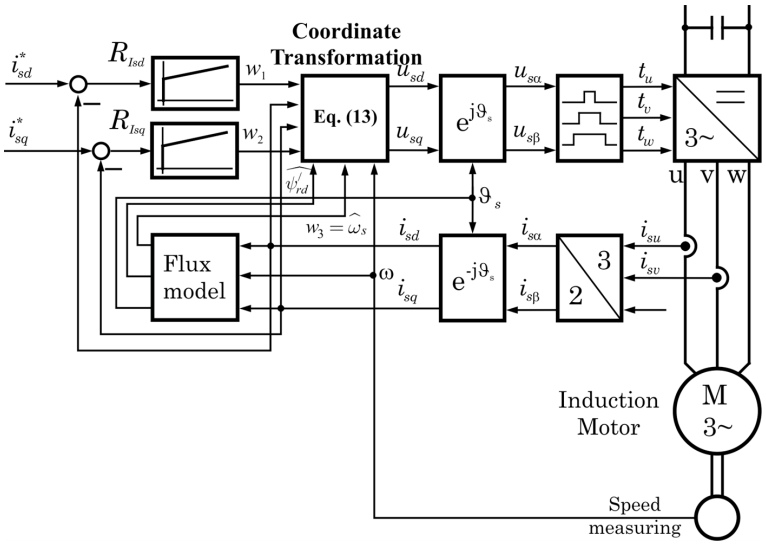

Figure 15: The new control structure of the inner loop with direct decoupling designed by using the method of exact linearization ([8])

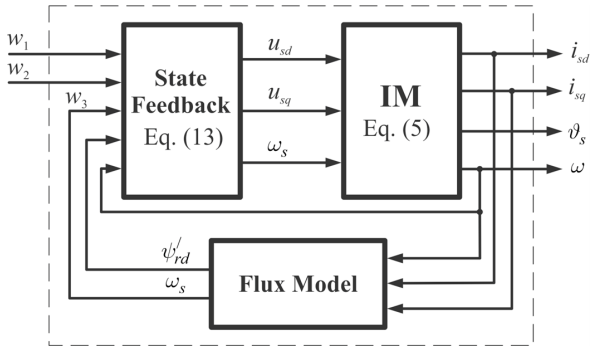

Figure 16: Substitute linear process model of the IM as starting point for controller design ([8])

In a more exact analysis the following essential knowledge can be learned:

- Besides the exact linearization achieved in the complete new state space $\mathbf{z}$, *the input-output decoupling relations are totally guaranteed.*
- The three transfer functions respectively contain only one element of integration.

3.2.2. Flatness-based control

Firstly, the controller design begins with proving that the motor meets the flatness conditions (17), (18) and the output vector $\mathbf{y} = \left[\omega,\ \psi_{rd}^{/}\right]$ is also flat. Then, the steps follow [8]:

- Design of set point trajectory $\mathbf{y}^* = \left[\omega^*,\ \psi_{rd}^{\prime *}\right]$.

- Design of feed-forward component $\mathbf{u}_s^f$ of the stator voltage vector $\mathbf{u}_s$.

$$\begin{cases} u_{sd}^f = \sigma L_s \left[\dfrac{di_{sd}^*}{dt} + \left(\dfrac{1}{\sigma T_s} + \dfrac{1-\sigma}{\sigma T_r}\right) i_{sd}^* - \omega_s^* i_{sq}^* - \dfrac{1-\sigma}{\sigma T_r}\psi_{rd}^{\prime *}\right] \\ u_{sq}^f = \sigma L_s \left[\dfrac{di_{sq}^*}{dt} + \omega_s^* i_{sd}^* + \left(\dfrac{1}{\sigma T_s} + \dfrac{1-\sigma}{\sigma T_r}\right) i_{sq}^* + \dfrac{1-\sigma}{\sigma}\omega^* \psi_{rd}^{\prime *}\right] \end{cases} \tag{25}$$

with $\omega_s^* = \omega^* + i_{sq}^* \Big/ \left(T_r \psi_{rd}^{\prime *}\right)$.

- Design of feedback component $\mathbf{u}_s^b$ of the stator voltage vector $\mathbf{u}_s$ (Figures 17 and 18).

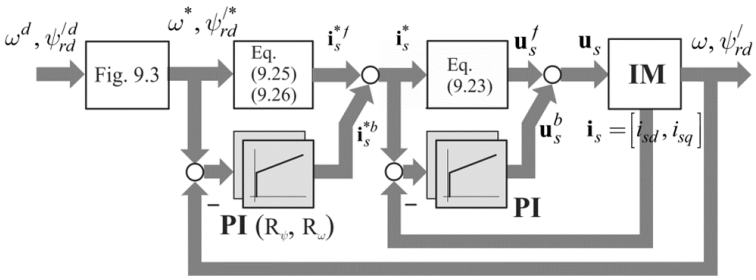

Figure 17: The block structure of the flatness-based IM control (concrete design steps can be seen in ([8])

.

For implementation, the block structure in Figure 17 is redrawn more concretely as in Figure 18. The flatness-based variant is characterized by high dynamics compared to other variants.

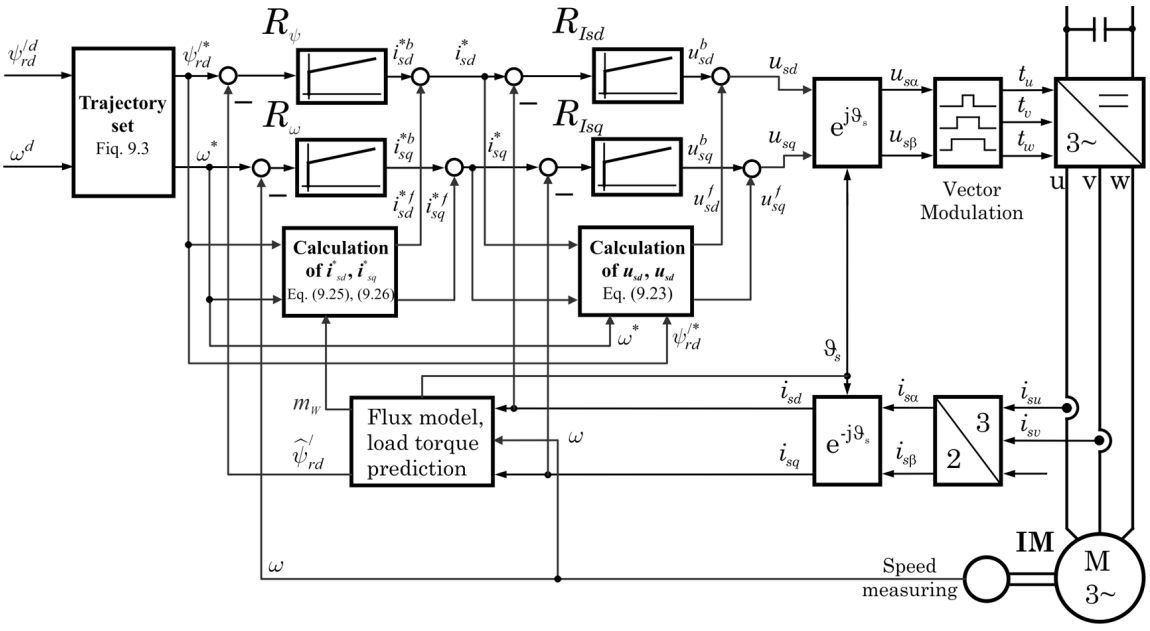

Figure 18: The detailed flatness-based cascaded control structure for IM drives ([8])

4. FOC-CONTROLLED THREE-PHASE AC DRIVE IN THE ROLE OF AN ACTUATOR

4.1. Two-mass system model

After torque m_M is generated with high dynamic drive quality (Figure 1) using the FOC-controlled innermost current control loop, the following question is how m_M can be provided to the work machine or the load side or load process. In many cases, it is sufficient to assume that the load side is connected to the motor side using an ideally rigid shaft (Figure 19a).

The starting point is the equation of motion of the system of equations describing the squirrel cage rotor induction motor

$$m_M = m_L + J\frac{d\omega}{dt}. \tag{26}$$

Equation (26) describes the rotational motion created by the motor for the working machine (load m_L) through the torque m_M with the ideal assumption: The motor shaft (inclusive rotor with inertial mass J_1) is ideally rigidly coupled with the working machine shaft (load with inertia J_2). Therefore, we can calculate the conversion of J_2 towards the motor shaft with $J = J_1 + J_2$. The term single-mass systems can be used to refer to this system.

However, in practice, that ideal situation rarely occurs. The coupling can be described as shown in Figure 19b below.

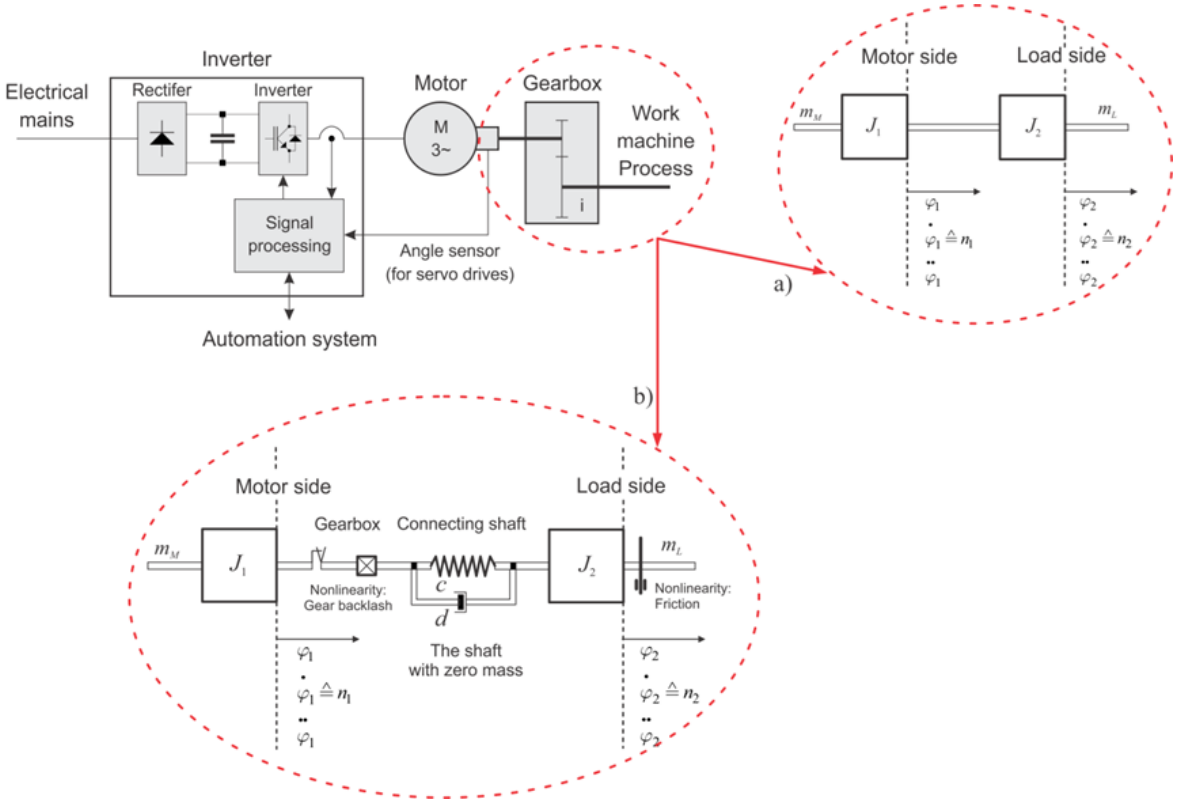

Figure 19: Coupling of the motor with the working machine in practice: a) rigid coupling; b) elastic coupling

Figure 19b illustrates the minimal typical structure of a transmission branch, briefly as follows. In the following instructions, we temporarily ignore the two nonlinear characteristics of gear backlash and friction. The following basic physical relationships will be used:

- Acceleration torque of the inertial mass J: $m_B = J\ddot{\varphi}$,
- Transmitted torque due to the elastic component c: $m_C = c\triangle\varphi$,
- Transmitted torque due to the damping component d: $m_D = d\triangle\dot{\varphi}$,

with

$\ddot{\varphi}$	Angular acceleration	
$\dot{\varphi}$	Angular velocity (rotational velocity)	
φ	Angle of rotation	
c	Rotary spring *stiffness*	Parameters of the connecting shaft
d	Mechanical *damping*	

It is known that the block structure of the two-mass system (Figure 19b) can be derived using the parameters defined above. Using the above relationships, we can easily write the *equation of motion at the locations* of the transmission branch as follows:

- On the side of the inertia mass J_1 of the drive motor rotor

$$\ddot{\varphi}_1 = \frac{1}{J_1} m_M - \frac{1}{J_1}(m_C + m_D). \tag{27}$$

- Connecting shaft between J_1 and J_2

$$\begin{aligned} \triangle\varphi &= \varphi_1 - \varphi_2, \\ \triangle\dot{\varphi} &= \dot{\varphi}_1 - \dot{\varphi}_2. \end{aligned} \tag{28}$$

- On the side of the working machine (the load) J_2

$$\ddot{\varphi}_2 = \frac{1}{J_2}(m_C + m_D) - \frac{1}{J_2} m_L. \tag{29}$$

- The torque components transmitted through the connecting shaft are calculated:

$$m_C + m_D = c\triangle\varphi + d(\dot{\varphi}_1 - \dot{\varphi}_2). \tag{30}$$

The *feedback torque component* according to (30) is substituted into the two equations of motion (27), (29). We obtain the following system of state equations (31)

$$\begin{cases} \ddot{\varphi}_1 & = -\frac{d}{J_1}\dot{\varphi}_1 - \frac{c}{J_1}\triangle\varphi + \frac{d}{J_1}\dot{\varphi}_2 + \frac{1}{J_1} m_M \\ \triangle\dot{\varphi} & = \dot{\varphi}_1 - \dot{\varphi}_2 \\ \ddot{\varphi}_2 & = \frac{d}{J_2}\dot{\varphi}_1 + \frac{c}{J_2}\triangle\varphi - \frac{d}{J_2}\dot{\varphi}_2 - \frac{1}{J_2} m_L. \end{cases} \tag{31}$$

Using equations (27)-(31), we can construct a structural diagram of a two-mass system with linear soft coupling, as shown in Figure 20.

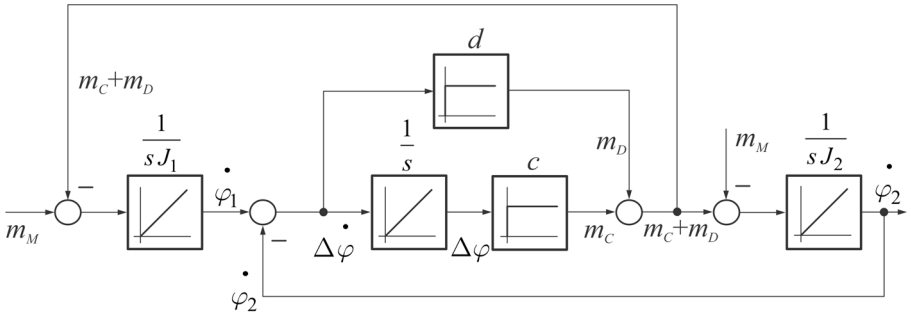

Figure 20: Block diagram structure of the two-mass system

4.2. State feedback control of two-mass systems

The system of equations (31) is rewritten as follows

$$\underbrace{\begin{bmatrix}\ddot{\varphi}_1\\ \triangle\dot{\varphi}\\ \ddot{\varphi}_2\end{bmatrix}}_{\dot{\mathbf{x}}} = \underbrace{\begin{bmatrix}-\frac{d}{J_1} & -\frac{c}{J_1} & -\frac{d}{J_1}\\ 1 & 0 & -1\\ \frac{d}{J_2} & \frac{c}{J_2} & -\frac{d}{J_2}\end{bmatrix}}_{\mathbf{A}} \underbrace{\begin{bmatrix}\dot{\varphi}_1\\ \triangle\varphi\\ \dot{\varphi}_2\end{bmatrix}}_{\mathbf{x}} + \underbrace{\begin{bmatrix}\frac{1}{J_1}\\ 0\\ 0\end{bmatrix}}_{\mathbf{b}} \underbrace{m_M}_{u} + \underbrace{\begin{bmatrix}0\\ 0\\ -\frac{1}{J_2}\end{bmatrix}}_{\mathbf{v}} \underbrace{m_L}_{z}$$

$$\dot{\mathbf{x}}(t) = \mathbf{A}\mathbf{x}(t) + \mathbf{b}u(t) + \mathbf{v}z(t) \tag{32}$$

In which $u(t)$ is the control variable and $z(t)$ is the disturbance variable. With model (32), we can design a structure to control the speed of the working machine (Figure 21).

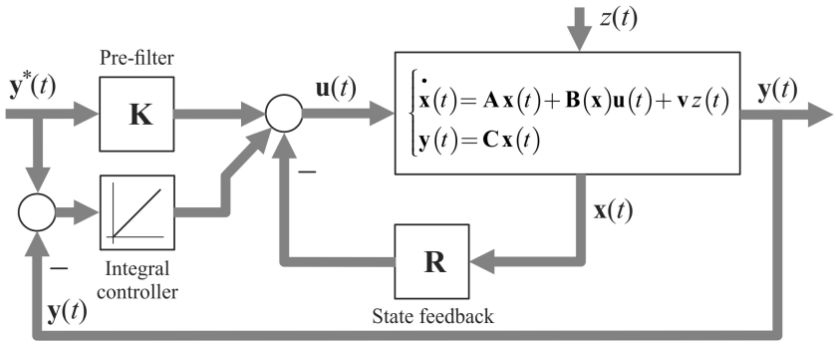

Figure 21: Block diagram structure of the two-mass system

4.2.1. State control in the nominal speed range

The main feature of the nominal speed range is that the motor is always magnetized to the nominal value. In other words, the rotor flux ψ_{rd} is always stably controlled to the nominal value and it *can be seen as a constant parameter*. Then, the torque m_M is directly proportional to the current i_{sq} and m_M is considered as the input control variable of the two-mass mechanical system. The stator current vector control loop is replaced by the PT_1 stage as shown in Figure 22.

Figure 22 illustrates the advantage of considering the constantly controlled rotor flux as a parameter so that the system order is reduced from 4 to 3.

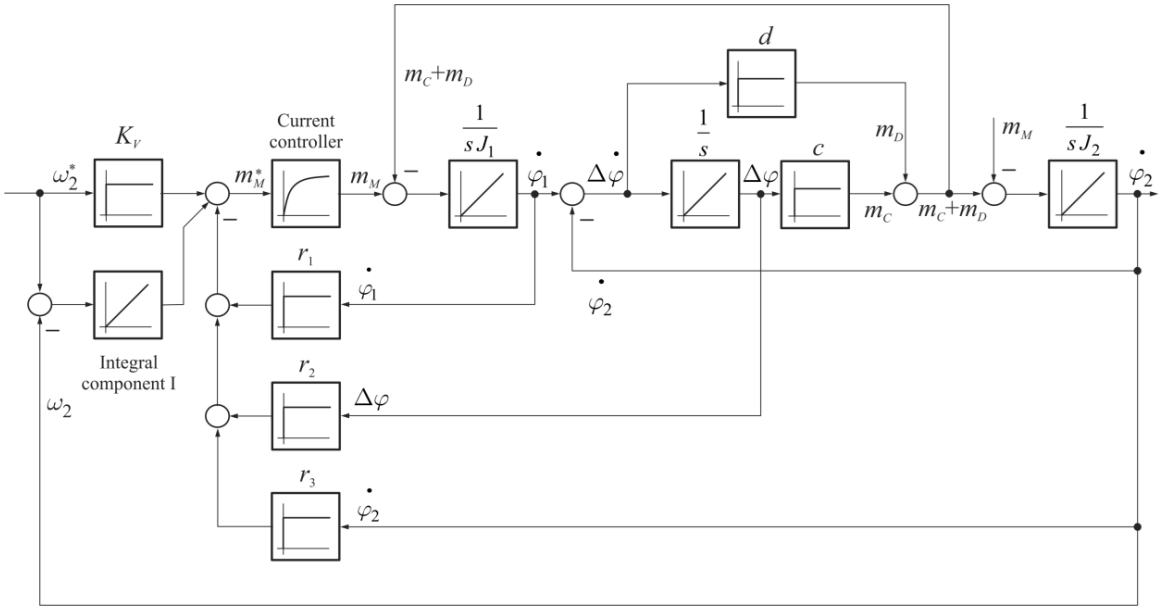

Figure 22: The load-side speed control structure on the state space in the nominal speed range

4.2.2. State control in the speed range with field weakening

Assumed, the drive system is operated at a speed outside the nominal range (area with field weakening). In this range, the rotor flux ψ_{rd} is no longer considered constant, but is controlled so that it changes with the dynamics of the speed of the motor shaft $\omega_1 = \dot{\varphi}_1$. When replacing $m_M = k_\omega i_m i_{sq}$, the equation of motion on the J_1 inertia block side of the drive motor (27) is rewritten as follows

$$\ddot{\varphi}_1 = \frac{1}{J_1} k_\omega i_m i_{sq} - \frac{1}{J_1}(m_C + m_D), \;\; k_\omega = \frac{3}{2}\frac{Z_p L_m^2}{L_r}. \tag{33}$$

In (33), $i_m = \psi_{rd}/L_m$ is the magnetization current with the magnetization process described by the following relationship

$$\dot{i}_m = -\frac{1}{T_r} i_m + \frac{1}{T_r} i_{sd}. \tag{34}$$

Combining (32) with (33) and (34), we have the full state model of the electro-mechanical system as follows

$$\underbrace{\begin{bmatrix} \dot{i}_m \\ \ddot{\varphi}_1 \\ \triangle\dot{\varphi} \\ \ddot{\varphi}_2 \end{bmatrix}}_{\dot{\mathbf{x}}} = \underbrace{\begin{bmatrix} \frac{1}{T_r} & 0 & 0 & 0 \\ 0 & -\frac{d}{J_1} & -\frac{c}{J_1} & \frac{d}{J_1} \\ 0 & 1 & 0 & -1 \\ 0 & \frac{d}{J_2} & \frac{c}{J_2} & -\frac{-d}{J_2} \end{bmatrix}}_{\mathbf{A}} \underbrace{\begin{bmatrix} i_m \\ \dot{\varphi}_1 \\ \triangle\varphi \\ \dot{\varphi}_2 \end{bmatrix}}_{\mathbf{x}} + \underbrace{\begin{bmatrix} \frac{1}{T_r} & 0 \\ 0 & \frac{K_\omega i_m}{J_1} \\ 0 & 0 \\ 0 & 0 \end{bmatrix}}_{\mathbf{B(x)}} \underbrace{\begin{bmatrix} i_{sd} \\ i_{sq} \end{bmatrix}}_{u} + \underbrace{\begin{bmatrix} 0 \\ 0 \\ 0 \\ -\frac{1}{J_2} \end{bmatrix}}_{\mathbf{v}} \underbrace{m_L}_{z}$$

$$\underbrace{\begin{bmatrix} i_m \\ \dot{\varphi}_2 \end{bmatrix}}_{\mathbf{y}} = \underbrace{\begin{bmatrix} 1 & 0 & 0 & 0 \\ 0 & 0 & 0 & 1 \end{bmatrix}}_{\mathbf{C}} \underbrace{\begin{bmatrix} i_m \\ \dot{\varphi}_1 \\ \triangle\varphi \\ \dot{\varphi}_2 \end{bmatrix}}_{\mathbf{x}},$$

$$\begin{cases} \dot{\mathbf{x}}(t) &= \mathbf{A}x(t) + \mathbf{B}(\mathbf{x})u(t) + \mathbf{v}z(t) \\ \mathbf{y}(t) &= \mathbf{C}x(t). \end{cases} \tag{35}$$

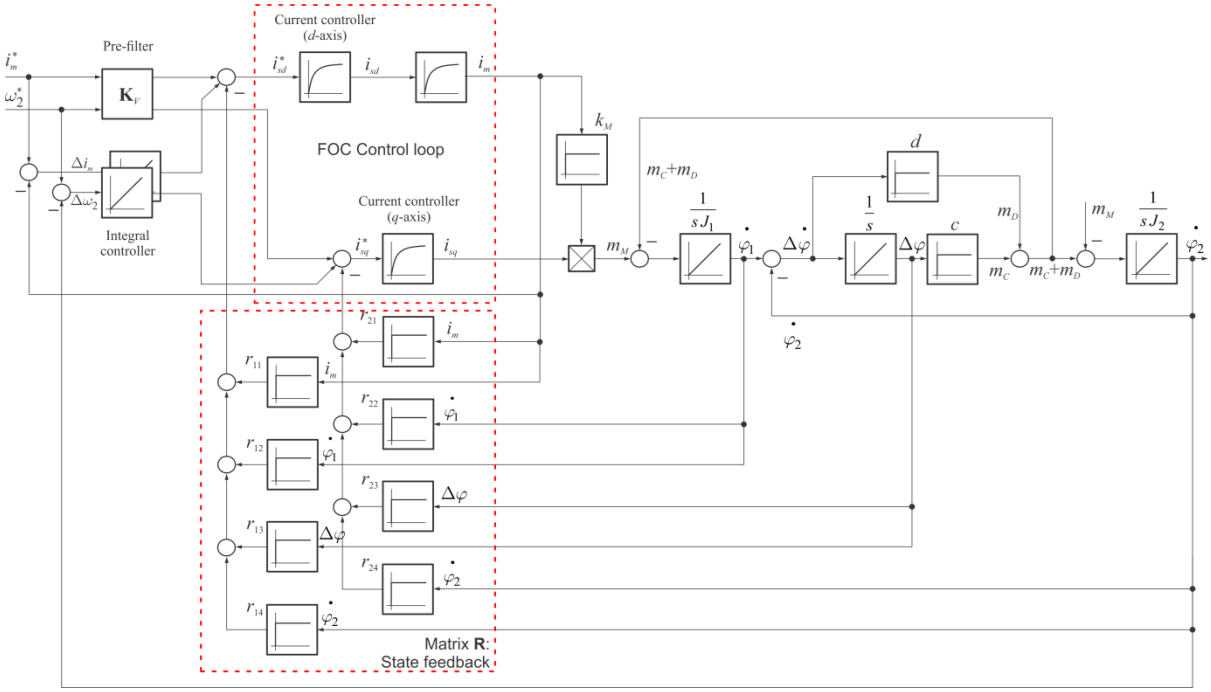

Figure 23: The load-side speed control structure on the state space with field weakening

The model (35) of the electro-mechanical system has the following main characteristics:

- The drive system has a current control circuit that meets the requirements of "fast – precise – decoupled". It can therefore be approximated by a dead time term or a first-order delay PT1, as shown in Figures 21 and 22.
- The model contains a term $\mathbf{B(x)u(t)}$, reflecting bilinear nonlinear characteristics (the product between the state variable i_m and the input variable i_{sq}).
- The nonlinear model (35) is the starting point for designing nonlinear controllers for the rotational speed of electro-mechanical systems (inverters, motors, working machines), especially important when the motor needs to be operated at a speed range above the nominal speed (range with field weakening).
- Model (35) is also the starting point for designing the necessary observer for the two-mass system.

5. CONCLUSION

On the occasion of the FOC - Field Oriented Controlled - turning 50 years old 1973 - 2023, it has gone through 50 years of "Research - Development - Application" to become the most popular method

in the industry. In the era of the 4th Industrial Revolution, when the entire society is passionately talking about AI or IoT, the article helps review the level of development of FOC. Paper content includes:

- Summary of the *idea of vector-based control* and the FOC method.
- *Modeling* of a three-phase squirrel-cage induction motor.
- *Fast torque impression* using dynamic current feedback control.
- FOC controlled 3-phase AC drive in the *role of an actuator* moving the load.

With content in the form of "State of the Art", the article hopes to provide readers with a general view of the group of problems that need to be solved when drive problems appear in practice.

REFERENCES

[1] K. Hasse, "On the dynamics of speed-controlled drives with converter-fed asynchronous squirrel-cage machines," German PhD Thesis, University Darmstadt, 1969.

[2] F. Blaschke, "The principle of field orientation, as applied to the new transvector-closed loop control systems for rotating field machines," *Siemens Review,* p. 217, 1972.

[3] W. Leonhard, "30 Years Space Vectors, 20 Years Field Orientation, 10 Years Digital Signal Processing with Controlled AC-Drives, a Review," *EPE Journal,* Part 1, vol. 1, no. 1, July 1991, pp. 13–19. DOI: 10.1080/09398368.1991.11463257; Part 2, vol. 1, no. 2, October 1991, pp. 89–101. DOI: 10.1080/09398368.1991.11463267

[4] E. Kiel (Editor) et al, *Drive Solutions - Mechatronics for Production and Logistics,* Springer Verlag Berlin Heidelberg NewYork, 2007.

[5] N.P. Quang, *Practice of Field-Oriented Three-phase AC Drive Controls.* German Publishing House Expert, 1993.

[6] N.P. Quang, R. Wirfs, "Multi-variable controller replaces PI controller: An inverter concept for three-phase AC drives," *German Electronik,* vol. 7, pp. 106-110, 1995.

[7] N.P. Quang, "Multi-variable controller replaces PI controller: From parameters to programmable controller equations," *German Electronik*, vol. 8, pp. 112-120, 1996.

[8] N.P. Quang, J.A. Dittrich, *Vector Control of Three-Phase AC Machines – System Development in the Practice,* Springer Berlin Heidelberg, 2nd Edition, 2015.

[9] M. Fliess, J. Lévine, P. Martin, and P. Rouchon, "A Lie-Backlund approach to equivalence and flatness of nonlinear systems," in *IEEE Transactions on Automatic Control,* vol. 44, no. 5, pp. 922-937, May 1999, Doi: 10.1109/9.763209

[10] J. Lévine, *Analysis and Control of Nonlinear Systems – A Flatness-based Approach.* Springer Dordrecht Heidelberg London New York, 2009.

[11] N.P. Quang and R. Schönfeld, "Dynamic current control for torque impression in three-phase AC drives with pulse inverters," *German Archive of Electrical Engineering,* vol. 76, pp. 317-323, 1993.

[12] N.P. Quang, R. Schönfeld, "A current vector control with finite response time for dynamic three-phase AC drives," *German Archive of Electrical Engineering,* vol. 76, pp. 377-385, 1993.

[13] N.P. Quang, V.T. Ha, and T.V. Trung, "A new control design with dead-beat behavior for stator current vector in three-phase AC drives," *SSRG International Journal of Electrical and Electronics Engineering IJEEE,* vol. 5, no. 4, pp. 1-5, April 2018.

[14] F. Khorrami, P. Krishnamurthy, and H. Melkote, *Modeling and Adaptive Nonlinear Control of Electric Motors.* Springer Berlin Heidelberg New York, 2003.

[15] R. Ortega, A. Loría, P.J. Nicklasson, and H. Sira-Ramírez, *Passivity-based Control of Euler-Lagrange Systems: Mechanical, Electrical and Electromechanical Applications.* Springer London Berlin Heidelberg, 1998.

[16] M. Bodson and J. Chiasson, "Differential-Geometric Methods for Control of Electric Motors," *Intern. Journal Robust Nonlinear Control,* vol. 8, no. 11, pp. 923-954, 1998. https://doi.org/10.1002/(SICI)1099-1239(199809)8:11<923::AID-RNC369>3.0.CO;2-S

[17] W. Leonhard, *Control of Electrical Drives,* Springer Verlag Berlin Heidelberg NewYork, 3rd Edition, 2001.

Received on Octorber 18, 2023
Accepted on November 09, 2023